Temporal variations in $^{87}Sr/^{86}Sr$ and ε_{Nd} in sediments of the southeastern Arabian Sea: Impact of monsoon and surface water circulation

Vineet Goswami, Sunil K. Singh, Ravi Bhushan, and Vinai K. Rai

Physical Research Laboratory, Ahmedabad 380 009, India (vineetg@prl.res.in; sunil@prl.res.in; bhushan@prl.res.in; rai@prl.res.in)

[1] Sr and Nd isotopic composition of silicate fractions of sediments have been measured in two well dated gravity cores from the eastern Arabian Sea archiving a depositional history of ~29 and ~40 ka. The $^{87}Sr/^{86}Sr$ and ε_{Nd} in the northern core (SS-3104G; 12.8°N, 71.7°E) ranges from 0.71416 to 0.71840 and −8.8 to −12.8; these variations are limited compared to those in the southeastern core (SS-3101G; 6.0°N, 74.0°E), in which they vary from 0.71412 to 0.72069 and −9.0 to −15.2 respectively. This suggests that the variation in the relative proportions of sediments supplied from different sources to the core SS-3104G are limited compared to core SS-3101G. The $^{87}Sr/^{86}Sr$ and ε_{Nd} profiles of SS-3101G exhibit two major excursions, ca. 9 ka and 20 ka, coinciding with periods of Holocene Intensified Monsoon Phase (IMP) and the Last Glacial Maximum (LGM) respectively with more radiogenic $^{87}Sr/^{86}Sr$ and lower ε_{Nd} during these periods. These excursions have been explained in terms of changes in the erosion patterns in the source regions and surface circulation of the Northern Indian Ocean resulting from monsoon intensity variations. The intensification of North-East (NE) monsoon and associated strengthening of the East Indian Coastal Current in southwest direction during LGM transported sediments with higher $^{87}Sr/^{86}Sr$ and lower ε_{Nd} from the western Bay of Bengal to the Arabian Sea. In contrast, enhanced South-West (SW) monsoon at ~9 ka facilitated the transport of sediments from the northern Arabian Sea, particularly Indus derived, to the southeastern Arabian Sea. This study thus highlights the impact of monsoon variability on erosion patterns and ocean surface currents on the dispersal of sediments in determining the Sr and Nd isotopic composition of sediments deposited in the eastern Arabian Sea during the last ~40 ka.

1. Introduction

[2] The Arabian Sea annually receives ~400 million tons of suspended load from the Himalaya and Transhimalaya [*Milliman et al.*, 1984] through the Indus river system, and ~100 million tons through the Narmada, Tapi and the rivers of the Western Ghats [*Alagarsamy and Zhang*, 2005;

Chandramohan and Balchand, 2007]. In addition, ~100 million tons of aeolian dust from the deserts of Oman, Africa and western India is deposited annually in the Arabian Sea, its contribution to the eastern Arabian Sea being only ~30 million tons, which further decreases toward the Indian peninsula [*Ramaswamy and Nair*, 1994; *Sirocko and Sarnthein*, 1989]. The sediments deposited in the Arabian Sea preserve in them the records of erosional patterns in their source regions, factors regulating them and the pathways of sediment dispersal in the sea [*Clift et al.*, 2008; *Rahaman et al.*, 2009].

[3] One of the key factors determining the erosion patterns of the drainage basins is the monsoon. The Indian subcontinent experiences two monsoons annually, the South-West (summer) and the North-East (winter) monsoons; the former being more pronounced at present. The intensities and patterns of these monsoons have varied during the past [*Fleitmann et al.*, 2003; *Gupta et al.*, 2003; *Herzschuh*, 2006], these in turn, have affected the erosion distribution of drainage basins [*Clift et al.*, 2008; *Rahaman et al.*, 2009] and supply of sediments to the seas around India [*Ahmad et al.*, 2005; *Colin et al.*, 1999; *Tripathy et al.*, 2011]. These variations, in addition to impacting erosion, also influence the surface water circulation in the Arabian Sea and the Bay of Bengal which determine the sediment dispersal and deposition in them. During the SW monsoon, surface water from the Arabian Sea flows to the Bay of Bengal; in contrast, during the NE monsoon, surface currents flow from the Bay of Bengal to the Arabian Sea [*Schott and McCreary*, 2001; *Shankar et al.*, 2002]. There is evidence to suggest that the transport of low-salinity water from the Bay of Bengal to the Arabian Sea was enhanced during the Last Glacial Maximum (LGM) due to a more intense NE monsoon [*Sarkar et al.*, 1990; *Tiwari et al.*, 2005].

[4] Clay mineralogy and radiogenic isotopes of Sr and Nd have been used to investigate spatial variations in the provenance of sediments in the Arabian Sea and the Bay of Bengal and their causative factors. For example, investigations of surface sediments in the Arabian Sea suggest that supply from the Himalaya, Transhimalaya and Karakorum ranges brought via the Indus dominate in the northern and central regions [*Garzanti et al.*, 2005], whereas the sediments off the shelf and slope regions of the eastern Arabian Sea are sourced mainly from peninsular India [*Chauhan and Gujar*, 1996; *Chauhan et al.*, 2010; *Kessarkar et al.*, 2003; *Kolla et al.*, 1976; *Rao and Rao*, 1995]. There is also evidence

based on clay mineral studies of sediments from the southwestern slope of India that suggest long range transport of Ganga-Brahmaputra sediments to the tip of Indian peninsula by surface currents [*Chauhan and Gujar*, 1996; *Chauhan et al.*, 2010].

[5] The radiogenic isotopes of Sr and Nd in silicate phases are commonly used as proxies for sediment provenances. The Sr (^{87}Sr/^{86}Sr) and Nd (^{143}Nd/^{144}Nd) isotopic composition of continental source rocks depend on their Rb/Sr and Sm/Nd ratios and their ages. Terrigenous sediments in the ocean are weathering products of continental rocks that have wide range of Sr and Nd isotope ratios. Thus, the Sr and Nd isotopic composition of detrital marine sediments provide a means to trace their sources and their variations in space and time [*Innocent et al.*, 2000; *Rutberg et al.*, 2005].

[6] The objective of this work is to track the temporal variation in the provenance of sediments deposited in the eastern region of the Arabian Sea during the last ~40 ka and assess the impact of climate and surface water circulation in determining their source(s) and dispersal. This work also addresses the issue of long range transport of sediments from the Bay of Bengal to the Arabian Sea during the LGM due to intensification of NE monsoon.

2. Study Area, Materials and Methods

2.1. Details of the Sediment Cores and Their Chronology

[7] Sediments from two gravity cores; SS-3101G and SS-3104G, raised from the southeastern Arabian Sea (Figures 1 and 2 and Table S1 in the auxiliary material) onboard FORV Sagar Sampada during 1991–92 [*Somayajulu et al.*, 1999] are investigated for their Sr and Nd isotopes of silicate phases in this study.[1] These cores have been studied in detail earlier to retrieve records of paleoproductivity and monsoon using a multiproxy approach [*Agnihotri et al.*, 2003; *Sarkar et al.*, 2000]. These two cores have been selected for this study as (1) their chronology is well established based on AMS ^{14}C dating of planktonic foraminiferal separates (Table S2) [*Agnihotri*, 2001; *Agnihotri et al.*, 2003; *Somayajulu et al.*, 1999], which show that they represent depositional histories of ~29 and ~40 ka and (2) they are strategically located to investigate the impact of SW/NE monsoon variations on the transport of sediments from the Bay of Bengal

---

[1]Auxiliary materials are available in the HTML. doi:10.1029/2011GC003802.
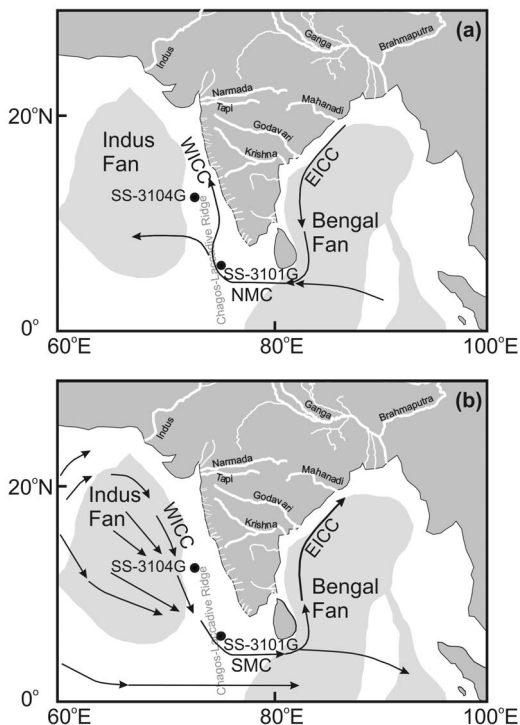
Figure 1. Locations of the two sediment cores analyzed in the study. Various rivers draining into the Arabian Sea and the Bay of Bengal are also shown. Core SS-3101G lies between the present-day limits of the Indus and Bengal Fans. Core SS-3104 lies in the present-day Deccan basaltic provenance zone and outside the limit of Indus Fan. The arrows indicate the direction of surface currents during the intensification of (a) North-East monsoon and (b) South-West monsoon; [*Schott and McCreary*, 2001; *Shankar et al.*, 2002; *Wyrtki*, 1973]. NMC, North-East Monsoon Current; SMC, South-West Monsoon Current; EICC, East India Coastal Current; WICC, West India Coastal Current.

to the Arabian Sea. The core SS-3101G is located east of Chagos Laccadive Ridge adjacent to a sill and is in the pathway of water exchange between the Bay of Bengal and the Arabian Sea due to monsoon pattern reversal (Figure 1). The average sediment accumulation rates of these cores are 4.6 and 3.5 cm/ka respectively, with higher rates 7.5 and 4.2 cm/ka prior to LGM which decreased to 2.9 and 2.7 cm/ka after the LGM (Figure S1). The sedimentation rates of both these cores were higher during LGM [*Agnihotri*, 2001; *Agnihotri et al.*, 2003; *Somayajulu et al.*, 1999].

2.2. River Sediments

[8] The Arabian Sea receives detrital sediments from several rivers. Sr and Nd isotopic composition of these river sediments can serve as tracers to track

the provenance of sediments in the Arabian Sea. Such data are unavailable for the rivers from the western India such as the Narmada, Tapi, Nethravathi, Periyar and those draining the Western Ghats (Vashishthi, Kajli, and Sukh). Therefore, sediments from these rivers were collected and analyzed for Sr and Nd isotopic composition. The river sediments were generally collected from locations close to their mouths. The details of sampling locations of the river sediments and lithology of the river basins are given in Table S3.

[9] The sampling of the Mahi, Narmada and Tapi sediments was done in March, 2011; whereas for the Nethravathi, it was done during two different seasons, April and December, 2010. Samples of Periyar River sediments were collected from two locations, Cheranellur and Chennur (near Kochi), in April, 2011. The samples from the minor streams Vashishthi, Kajli, and Sukh flowing through the Western Ghats are from the collection of *Das et al.* [2005].
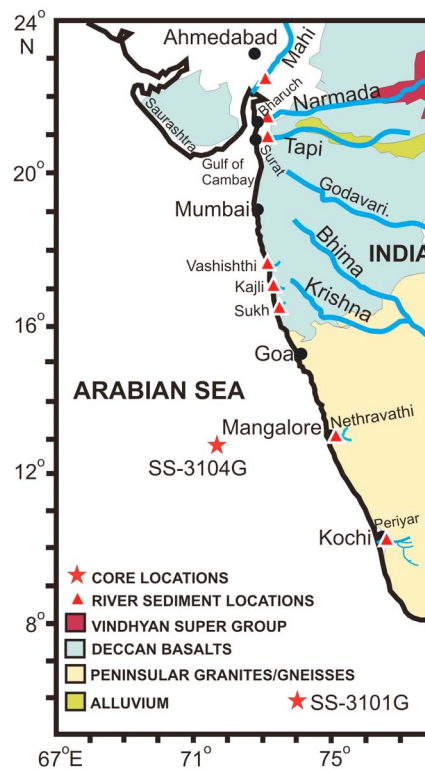

Figure 2. Sampling locations of sediments from rivers Mahi, Narmada, Tapi, Nethravathi, Periyar and the three Western Ghats streams Vashishthi, Kajli and Sukh. Broad lithology of the regions drained by these rivers and locations of cores SS-3101G and SS-3104G are also shown.

[10] The Mahi River drains a multilithological terrain composed of sediments of the Vindhyan Super Group, metamorphic rocks of the Aravalli Super Group, the Deccan basalts and the alluvial deposits of Pleistocene and Holocene ages [*Sridhar*, 2008]. The Narmada is the largest river draining into the Arabian Sea from western India. It passes through the Vindhyan ranges and Deccan basalts before plunging into the Arabian Sea at the Gulf of Cambay, near the town of Bharuch [*Gupta et al.*, 2011]. The Tapi River is the second largest west-flowing river; its drainage basin consists of Deccan basalts and alluvial deposits. The Tapi enters the Arabian Sea at the Gulf of Cambay near the city of Surat [*Kale et al.*, 2003]. The Nethravathi River is a minor river flowing through the Western Ghats draining granites/gneisses of peninsular India. It joins the Arabian Sea near Mangalore. The Periyar River drains crystalline rocks of Archaen age; sedimentary rocks of different ages and laterites capping them [*Chandramohan and Balchand*, 2007]. There are several small streams that drain Deccan basalts on the Western Ghats. In the present study sediment samples from three of these streams (Vashishthi, Kajli, and Sukh) were analyzed [*Das et al.*, 2005].

2.3. Measurement of Sr, Nd Concentrations and Isotopic Composition

[11] In the laboratory, the sediment samples were dried at 90°C for a few days, powdered using an agate mortar and pestle to less than 100 μm size and stored in pre-cleaned plastic containers.

[12] Sr and Nd isotopic analyses were made on carbonate and organic matter free fraction of the sediments [*Singh et al.*, 2008]. The powdered sediment samples were first decarbonated by leaching with 0.6 N HCl at 80°C for ~30 min with ultrasonic treatment. The slurry was centrifuged, residue washed with Milli-Q water, dried and ashed at ~600°C to oxidize organic matter. A known weight (~100 mg) of the carbonate and organic matter free fraction of the sediment was transferred to Savillex® vial and digested repeatedly with HF- HNO_3-HCl at ~120°C to bring the sediment to complete solution. The acid digestion step was repeated as needed to ensure that the entire sample was brought to complete solution. Sediments from the Arabian Sea were digested in the presence of ^{84}Sr and ^{150}Nd spikes whereas the river sediments were not spiked. Pure Sr and Nd fractions were separated from the solution following standard ion exchange procedures [*Rahaman et al.*, 2009; *Singh et al.*, 2008].

[13] Sr and Nd concentrations and ^{87}Sr/^{86}Sr and ^{143}Nd/^{144}Nd of the Arabian Sea sediments were measured on an Isoprobe-T TIMS and that of river sediments on a Finnigan Neptune MC-ICP-MS at PRL. The analyses were made in static multi-collection mode. Mass fractionation corrections for Sr and Nd were made by normalizing ^{86}Sr/^{88}Sr to 0.1194 and ^{146}Nd/^{144}Nd to 0.7219 respectively. During the course of analyses, NBS987 Sr standard was measured on both TIMS and MC-ICP-MS, these yielded values of 0.710227 ± 0.000014 (1σ, n = 110; σ = Standard Deviation) and 0.710287 ± 0.000020 (1σ, n = 15) respectively for ^{87}Sr/^{86}Sr. For Nd, JNdi-1 Nd standard was measured on TIMS which gave an average value of 0.512108 ± 0.000008 (1σ, n = 35) for ^{143}Nd/^{144}Nd, while JMC-321 standard was measured on MC-ICP-MS, this yielded an average value of 0.511095 ± 0.000007 (1σ, n = 13).

[14] The internal reproducibility of measurements was better than 10 ppm (1σ_μ) for both Sr and Nd isotopic ratios. Based on replicate measurements, the average variation between sets of repeats was determined to be 0.0002 and 0.00001 for ^{87}Sr/^{86}Sr and ^{143}Nd/^{144}Nd respectively. The Nd isotopic data is expressed in terms of standard ε notation,

$$\varepsilon_{Nd} = \left[\frac{^{143}Nd/^{144}Nd}{^{143}Nd/^{144}Nd_{CHUR}} - 1 \right] \times 10^4$$

where ^{143}Nd/^{144}Nd is the measured Nd isotopic composition of the sample and ^{143}Nd/^{144}Nd$_{CHUR}$ is the present-day ^{143}Nd/^{144}Nd value of CHUR (Chondritic Uniform Reservoir) which is 0.512638 [*Jacobsen and Wasserburg*, 1980]. The average variation between sets of repeats for ε_{Nd} was 0.2.

[15] Several total procedural blanks for Sr and Nd were also processed during the analysis. These blanks are several orders of magnitude lower than typical total Sr and Nd loads analyzed and hence no corrections for blanks were made.

3. Results

3.1. River Sediments

[16] The Sr and Nd isotopic composition in silicate fraction of river sediments are given in Table 1 and plotted in Figure 3. The isotopic composition of river sediments, as expected, reflects those of lithologies of the region. Sediment from the Mahi river is the most radiogenic in Sr (^{87}Sr/^{86}Sr = 0.73051) while its ε_{Nd} is quite unradiogenic (−20.3), consistent with the lithology of the Mahi

Table 1. Sr and Nd Isotopic Composition of Silicate Fraction of River Sediments[a]

Sample Code	River	$^{87}Sr/^{86}Sr$	$^{143}Nd/^{144}Nd$	ε_{Nd}
MH	Mahi	0.73051	0.51160	−20.3
NM	Narmada	0.72126	0.51203	−11.9
NM R	Narmada (Repeat)	0.72121	0.51205	−11.5
TP-1	Tapi	0.70947	0.51235	−5.7
TP-2	Tapi	0.70961	0.51233	−5.9
NETHRAVATHI-1	Nethravathi	0.72176	0.51054	−40.8
NETHRAVATHI-2	Nethravathi	0.71507	0.51097	−32.6
PERIYAR-1	Periyar	0.72379	0.51130	−26.2
PERIYAR-2	Periyar	0.72176	0.51119	−28.2
KJL/2K1/M	Kajli	0.70529	0.51275	2.2
SUKH/2K1/M	Sukh	0.70885	0.51257	−1.3
SUKH/2K1/M R	Sukh (Repeat)	0.70888	0.51258	−1.2
VAT/2K1/M	Vashishthi	0.70636	0.51258	−1.2

[a]Sampling location details are given in Table S3.

River basin that comprises of metamorphic rocks of the Aravalli Super Group, the Deccan basalts and the alluvial deposits of Pleistocene and Holocene ages. The $^{87}Sr/^{86}Sr$ and ε_{Nd} of the Narmada sediments are 0.72126 and −11.9 respectively, indicating contribution of radiogenic Sr from the Vindhyan Super Group along with unradiogenic Sr from Deccan basalts. The Deccan basalts comprise of various formation that are distinct in their Sr and Nd isotopic composition. The northern part of the Deccan basalts consists of Poladpur, Bushe and Jawhar-Igatpuri formations that show evidence of contamination with upper crustal material. The $^{87}Sr/^{86}Sr$ of these formations range from 0.705 to 0.720, whereas the ε_{Nd} varies from −5 to −20 [Mahoney et al., 2000; Peng et al., 1998]. The central and southwestern parts of the Deccan basalts are composed of the Ambenali and Mahabaleshwar formations that have less degree of crustal contamination. The $^{87}Sr/^{86}Sr$ and ε_{Nd} of these formations vary from 0.703 to 0.708 and +5 to −10 respectively [Mahoney et al., 2000; Peng et al., 1998]. The river Tapi flows through the northern areas of Deccan basalts; the Poladpur, Bushe and Jawhar-Igatpuri formations that are higher in $^{87}Sr/^{86}Sr$ and lower in ε_{Nd}. The two samples from the Tapi River yield $^{87}Sr/^{86}Sr$ of 0.70947, 0.70961 and ε_{Nd} of −5.9, −5.7; consistent with the isotopic composition of the dominant Deccan basalt formations in its drainage. The Nethravathi sediments collected in April, 2010 (Tables 1 and S3) have Sr isotopic composition (0.72176) and ε_{Nd} (−40.8) that are distinctively different from those in the sample collected in December, 2010 ($^{87}Sr/^{86}Sr$ 0.71507; ε_{Nd} −32.6; Table 1). These seasonal differences can arise from variations in mixing proportions of sediments from tributaries during different seasons. The isotopic composition of sediments of the Periyar River ($^{87}Sr/^{86}Sr$ 0.72379 and 0.72176; ε_{Nd} −26.2 and

−28.2; Table 1) is also close to that of the Nethravathi River, not unexpected considering that both of them drain Peninsular granites/gneisses. The Sr and Nd isotopic composition of sediments from the three Western Ghats streams are least radiogenic in $^{87}Sr/^{86}Sr$ (0.70529 to 0.70885) and most radiogenic in ε_{Nd} (−1.3 to 2.2), within the range reported for Deccan basalts.

3.2. Arabian Sea Sediments

[17] Sr and Nd concentrations and their isotopic compositions in the silicate fraction of sediments from SS-3104G and SS-3101G cores are given in Tables 2 and 3 and Figures 4 and 5 respectively. In SS-3104G, which lies in the northeastern Arabian Sea off Mangalore (Figures 1 and 2) the Sr and Nd concentrations range from 78 to 127 μg/g and 7 to 26 μg/g respectively and are generally lower than that in sediments of SS-3101G. The $^{87}Sr/^{86}Sr$ and
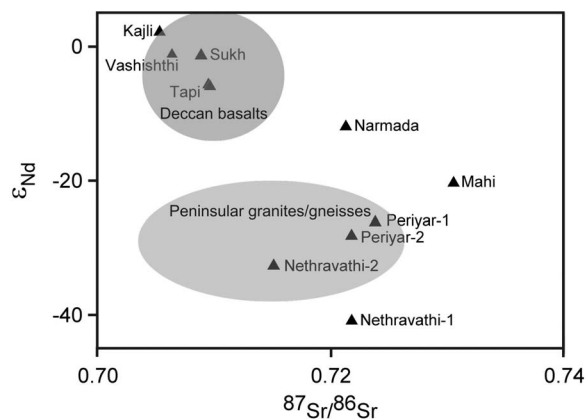

Figure 3. Sr-Nd isotope plot of contemporary river sediments (silicate fraction) draining into the Arabian Sea. The isotopic composition of major end-members is also given.

Table 2.   Sr and Nd Concentration and Isotopic Composition of Core SS-3104G Silicates[a]

Sample[b]	Age (ka)	Sr[c]	$^{87}Sr/^{86}Sr$[d]	Nd[c]	$^{143}Nd/^{144}Nd$[d]	ε_{Nd}
3104(2–3)	1.4	127.4	0.71416	15.5	0.51216	−9.4
3104(6–7)	1.6	84.3	0.71689	25.6	0.51198	−12.9
314(9–10)	3.3	88.7	0.71667	-	-	-
3104(11–12)	3.9	105.8	0.71521	-	-	-
3104(14–15)	4.9	-	-	14.4	0.51209	−10.7
3104(17–18)	5.8	86.9	0.71651	12.1	0.51213	−10.0
3104(19–20)	6.5	85.7	0.71658	11.1	0.51214	−9.6
3104(21–22)	7.6	88.6	0.71647	12.3	0.51213	−9.9
3104(23–24)	8.6	78.4	0.71648	9.9	0.51213	−9.9
3104(23–24)R	8.6	78.2	0.71621	10.9	0.51213	−9.9
3104(24–25)	9.2	111.3	0.71434	10.2	0.51219	−8.8
3104(26–27)	10.3	83.5	0.71702	12.3	0.51215	−9.5
3104(28–29)	11.4	86.5	0.71779	7.4	0.51207	−11.0
3104(30–31)	12.5	83.2	0.71748	9.3	0.51212	−10.2
3104(31–32)	13.0	94.1	0.71596	-	-	-
3104(32–33)	13.5	99.3	0.71671	13.5	0.51215	−9.5
3104(37–38)	15.5	100.1	0.71642	13.2	0.51214	−9.7
3104(37–38)R	15.5	100.1	0.71649	13.4	0.51214	−9.7
3104(41–42)	16.6	102.3	0.71698	14.0	0.51212	−10.1
3104(41–42)R	16.6	102.8	0.71687	14.8	0.51213	−9.9
3104(44–45)	17.4	96.6	0.71719	13.7	0.51211	−10.3
3104(48–49)	18.5	101.6	0.71773	14.3	0.51208	−10.8
3104(52–53)	19.6	98.5	0.71754	13.7	0.51210	−10.5
3104(61–62)	20.3	95.2	0.71745	12.6	0.51212	−10.0
3104(68–69)	20.8	93.6	0.71759	14.2	0.51214	−9.8
3104(71–72)	21.8	94.6	0.71788	12.8	0.51213	−9.9
3104(74–75)	22.8	-	-	14.7	0.51214	−9.7
3104(77–78)	23.8	-	-	13.8	0.51212	−10.2
3104(80–81)	24.8	91.4	0.71793	11.5	0.51211	−10.2
3104(82–83)	25.5	-	-	13.8	0.51209	−10.6
3104(84–85)	26.1	94.1	0.71840	14.0	0.51214	−9.8
3104(88–89)	26.7	93.8	0.71764	12.6	0.51213	−10.0
3104(95–96)	27.8	92.7	0.71708	8.6	0.51216	−9.3
3104(95–96)R	27.8	92.1	0.71693	-	-	-
3104(100–102)	28.9	111.2	0.71680	-	-	-
3104(102–104)	29.6	93.9	0.71768	13.9	0.51215	−9.6
3104(106–108)	30.9	94.9	0.71778	14.0	0.51214	−9.8
3104(114–116)	33.6	92.3	0.71785	13.4	0.51214	−9.8
3104(116–118)	34.3	112.2	0.71714	-	-	-
3104(122–124)	36.1	98.3	0.71649	14.4	0.51216	−9.3
3104(126–128)	37.1	112.6	0.71727	13.5	0.51214	−9.8
3104(126–128)R	37.1	111.0	0.71721	12.8	0.51215	−9.5
3104(132–134)	38.6	94.5	0.71702	13.4	0.51217	−9.0

[a]Abbreviations and symbols: -: not analyzed; R: Replicate analysis.
[b]Numbers in parenthesis are depth intervals in cm.
[c]Sr, Nd concentrations in $\mu g/g$.
[d]The errors on the Sr and Nd isotopic data are better than 10 ppm ($1\sigma_\mu$).

ε_{Nd} of SS-3104G (Table 2 and Figure 4) vary in a narrower range compared to SS-3101G, with most samples having $^{87}Sr/^{86}Sr$ between 0.716 to 0.718 and ε_{Nd} between −10.5 to −9.0. These ratios are within the range of isotopic compositions of slope sediments of west coast of India [*Kessarkar et al.,* 2003].

[18] In SS-3101G, from the near equatorial region (Figures 1 and 2) the Sr and Nd concentrations range from 94 to 200 $\mu g/g$ and 6 to 45 $\mu g/g$

respectively. Both $^{87}Sr/^{86}Sr$ (0.71412 to 0.72069) and ε_{Nd} (−15.2 to −9.0) show variations with depth but with opposite trends (Figures 5a and 5b).

[19] The concomitant temporal changes in both $^{87}Sr/^{86}Sr$ and ε_{Nd} in SS-3101G and the observation that their range is much larger than the average analytical uncertainty leads to infer that these variations represent source variability and/or their mixing proportions. Therefore, the data from these

Table 3. Sr and Nd Concentration and Isotopic Composition of Core SS-3101G Silicates[a]

Sample[b]	Age (ka)	Sr[c]	$^{87}Sr/^{86}Sr$[d]	Nd[c]	$^{143}Nd/^{144}Nd$[d]	ε_{Nd}
3101(1–2)	1.9	117.1	0.71631	19.8	0.51197	−13.0
3101(6–7)	3.3	156.4	0.71412	6.0	0.51213	−9.8
3101(10–11)	4.4	139.5	0.71459	8.7	0.51197	−13.1
3101(10–11)R	4.4	133.1	0.71501	-	-	-
3101(13–14)	5.5	112.7	0.71686	13.4	0.51194	−13.7
3101(16–17)	6.7	98.5	0.71838	12.7	0.51193	−13.8
3101(18–19)	7.5	95.7	0.71755	6.5	0.51192	−14.1
3101(21–22)	8.6	88.0	0.71930	12.5	0.51190	−14.4
3101(23–24)	9.4	107.9	0.71768	12.9	0.51190	−14.3
3101(26–27)	10.6	96.3	0.71677	11.7	0.51208	−10.9
3101(30–31)	11.6	203.3	0.71690	20.0	0.51206	−11.3
3101(34–35)	12.5	94.1	0.71830	13.7	0.51204	−11.8
3101(38–39)	13.5	98.3	0.71753	45.7	0.51218	−9.0
3101(41–42)	14.5	100.2	0.71685	12.8	0.51206	−11.2
3101(43–44)	15.1	109.1	0.71721	12.3	0.51204	−11.7
3101(46–47)	16.1	97.9	0.71776	19.6	0.51203	−11.8
3101(50–51)	17.4	95.9	0.71906	13.7	0.51200	−12.4
3101(53–54)	18.3	117.2	0.71773	-	-	-
3101(59–60)	19.1	101.1	0.72069	14.6	0.51189	−14.6
3101(62–63)	19.4	82.5	0.71949	13.4	0.51186	−15.2
3101(70–71)	20.4	90.4	0.71854	18.3	0.51196	−13.3
3101(86–87)	21.6	86.7	0.71920	17.4	0.51192	−14.0
3101(90–91)	22.3	101.2	0.71950	15.8	0.51192	−14.1
3101(90–91)R	22.3	101.9	0.71956	14.5	0.51190	−14.4
3101(94–95)	23.0	135.4	0.71805	-	-	-
3101(98–99)	23.7	113.0	0.71864	13.9	0.51194	−13.6
3101(102–104)	24.5	101.1	0.71752	11.3	0.51209	−10.7
3101(108–110)	25.4	102.8	0.71828	14.6	0.51206	−11.3
3101(116–118)	26.6	102.9	0.71779	13.1	0.51210	−10.6
3101(122–124)	27.5	94.7	0.71850	13.2	0.51208	−10.8
3101(126–128)	28.1	96.9	0.71860	13.8	0.51206	−11.3
3101(132–134)	29.0	95.2	0.71707	10.4	0.51206	−11.2

[a]Abbreviations and symbols: -: not analyzed; R: Replicate analysis.
[b]Numbers in parenthesis are depth intervals in cm.
[c]Sr, Nd concentrations in $\mu g/g$.
[d]The errors on the Sr and Nd isotopic data are better than 10 ppm ($1\sigma_\mu$).

two cores serve as a proxy to track variations in their provenance.

4. Discussion

[20] The Sr and Nd isotopic composition of river sediments supplied to the Arabian Sea are given in Figure 3. The data demonstrate the impact of various lithologies drained by these rivers in determining the isotopic composition of their sediments. The $^{87}Sr/^{86}Sr$ and ε_{Nd} values of the two Arabian Sea cores along with those of their potential sources, the Deccan basalts, the higher and lesser Himalaya, the Vindhyan Super Group and the Peninsular granites/gneisses are presented in an isotopic mixing diagram (Figure 6). Sr and Nd isotopic composition of these sources (Figure 6 and Table S4) are from published literature [*Ahmad et al.*, 2009; *Chakrabarti et al.*, 2007; *Clift et al.*, 2002, 2008,

2010; *Harris et al.*, 1994; *Peucat et al.*, 1989; *Singh et al.*, 2008; *Tripathy et al.*, 2011; *Tripathy*, 2011].

[21] The role of Indus as the source of sediments in the eastern Arabian Sea is debated. Based on clay mineralogical study, *Kessarkar et al.* [2003] suggest that the penetration of Indus sediments is restricted to the north of Saurashtra (~20°N), whereas *Ramaswamy and Nair* [1989] suggest that longshore current helps Indus sediments to be transported to the south of Mangalore.

[22] In addition to riverine particulates, another source of sediments to the Arabian Sea is aeolian dust from the deserts of Arabia [*Kolla et al.*, 1976; *Sirocko and Sarnthein*, 1989]. The magnitude of supply of dust has been reported to vary with time with enhanced contribution during the LGM [*Harrison et al.*, 2001; *Petit et al.*, 1999; *Reichart et al.*, 1997; *Sirocko et al.*, 2000]. The Sr and Nd isotopic composition of aeolian dust over the
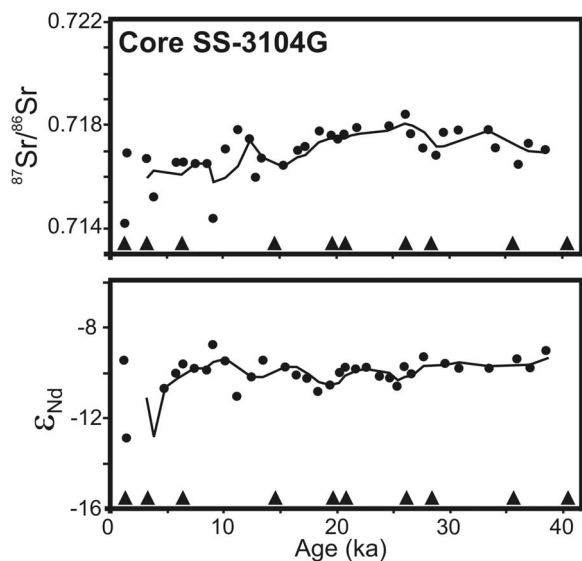
Figure 4. Temporal variation in $^{87}Sr/^{86}Sr$ and ε_{Nd} of sediments from SS-3104G. Sr and Nd isotope composition of these sediments display a narrow range, suggesting that their sources and the mixing proportions have remained nearly the same during the last 40 ka. The markers along the x axis of the plots show age control points in the core. The lines represent 3-point moving average of the data.

western Arabian Sea is characterized by unradiogenic Sr ($^{87}Sr/^{86}Sr = 0.709$) and radiogenic Nd ($\varepsilon_{Nd} = -6$) [*Sirocko*, 1995]. The Sr and Nd isotopic composition of dust falls within the range of Deccan basalts and if dust with such isotopic composition also deposits over the eastern Arabian Sea it is difficult to differentiate between aeolian dust and sediments sourced from basalts and assess their contribution. However, there have been earlier studies in the eastern Arabian Sea which suggest that aeolian dust is not a significant contributor of sediments to this area [*Kessarkar et al.*, 2003; *Kolla et al.*, 1976; *Sirocko and Sarnthein*, 1989].

4.1. Core SS-3104G

[23] The sediments of SS-3104G have $^{87}Sr/^{86}Sr$ and ε_{Nd} within a narrow range defined by the contemporary sediments of the Indus, Narmada, Tapi and other Western Ghats streams suggesting that all these rivers are potential sources of silicate sediments to this core site. Despite the proximity of Nethravathi River to the SS-3104G core site, its contribution and hence that from the Peninsular granites/gneisses to this core site seems minor. This inference is based upon the highly depleted ε_{Nd} values of the Nethravathi sediments and the observation that at present the Nethravathi River

supplies only ~1 million tons of sediments annually to the Arabian Sea [*Panda et al.*, 2011]. The limited range in Sr and Nd isotopic composition throughout the length of this core covering a time span of ~40 ka also leads us to infer that the provenance of sediments and their mixing proportion have remained nearly the same during this period. The reason for the lower $^{87}Sr/^{86}Sr$ in the (2–3) cm and ε_{Nd} in the (6–7) cm sections of SS-3104G (Table 2), however, is unclear.
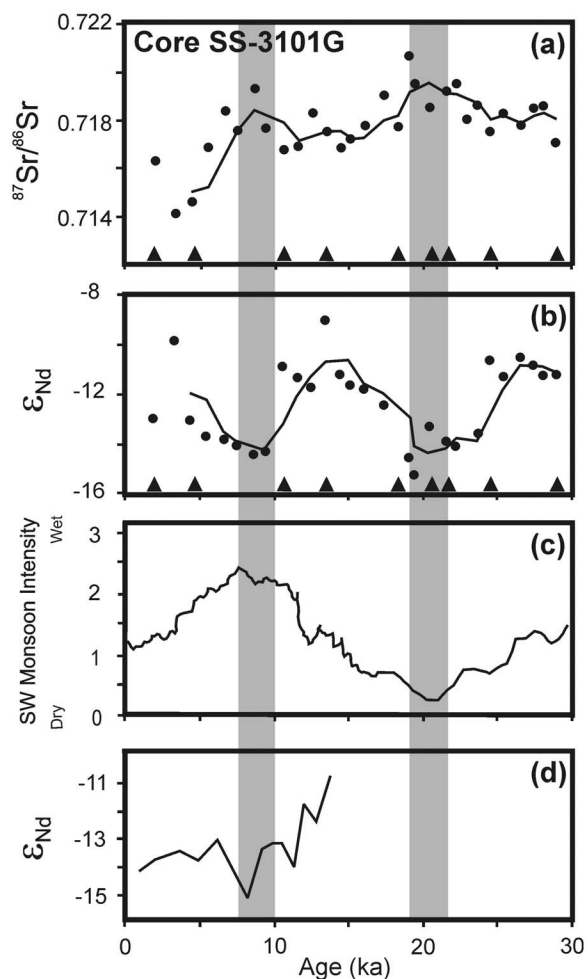

Figure 5. $^{87}Sr/^{86}Sr$ and ε_{Nd} of sediments of core SS-3101G. The data show significant temporal variation which correlate with (c) known climatic/monsoon variability [*Herzschuh*, 2006]. Sr and Nd isotope compositions of these sediments display two excursions during ~20 and ~9 ka coinciding with LGM and intensified SW monsoon. (a, b) The lines are 3-point moving average of the data respectively and the markers along the x axis of the plots show age control points in the core. (d) The line is 3-point moving average of ε_{Nd} values form the Indus delta [*Clift et al.*, 2008].
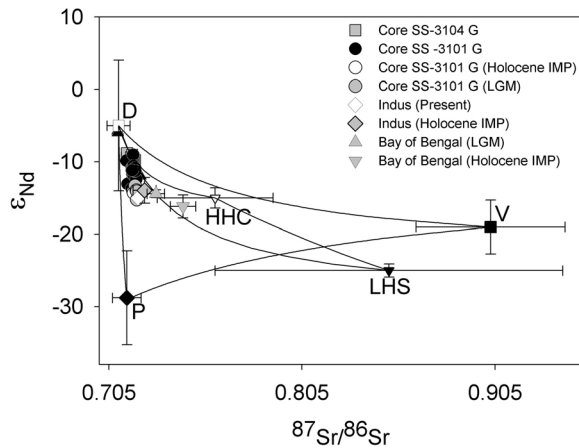
Figure 6. Sr and Nd isotope compositions of SS-3101G and SS-3104G sediments and their potential sources in two isotope mixing plot. Sediments of the core SS-3104G show very limited variation. Sr and Nd isotopic composition of SS-3101G sediments show wider range. Various lithologies used as end-members are: D, Deccan basalts; V, Vindhyan Super Group; P, Peninsular granites/gneisses; HHC, Higher Himalayan Crystalline; LHS, Lesser Himalayan Silicates.

4.2. Core SS-3101G

[24] The Sr and Nd isotopic composition of SS-3101G silicates displays wider range than those in SS-3104G with two excursions at ~9 ka and ~20 ka (Figures 5a and 5b). The lower bound of $^{87}Sr/^{86}Sr$ (i.e., the lowest values of $^{87}Sr/^{86}Sr$) and the upper bound of ε_{Nd} (i.e., the most radiogenic values of ε_{Nd}) of SS-3101G is similar to that observed for the core SS-3104G. Thus, the $^{87}Sr/^{86}Sr$ and ε_{Nd} of core SS-3104G can be considered to represent the baseline values of Sr and Nd isotopic composition of SS-3101G sediments. This in turn would suggest that Deccan basalts and the Vindhyan Super Group are the dominant sources of sediments to this core, delivered through the Narmada and the Tapi rivers. In addition, there has to be enhanced relative contribution of sediments with more radiogenic Sr and unradiogenic Nd to account for the excursions in its isotopic composition during ~9 ka and ~20 ka (Figure 5).

[25] The excursions in the Sr and Nd isotopic composition of SS-3101G core overlap with the known climatic (monsoon) variations in the Asian region (Figure 5c) [*Herzschuh*, 2006]. The timing of the first excursion in the Sr and Nd isotopic data at ~20 ka corresponds to the well known Last Glacial Maximum (LGM) whereas the excursion at ~9 ka overlaps with the known intensification of SW monsoon precipitation [*Fleitmann et al.*, 2003;

Herzschuh, 2006; *Prell and Kutzbach*, 1987; *Sinha et al.*, 2005]. It is clear from the observed inter-relations between Sr-Nd isotopic composition and monsoon variations (Figure 5) that climate exerts a significant control on the erosion patterns and sediment fluxes from different sources depositing at this core location and their mixing proportions.

4.2.1. Provenance of Sediments During Last Glacial Maximum (LGM)

[26] The Sr and Nd isotopic composition in SS-3101G during LGM show a peak in $^{87}Sr/^{86}Sr$ and a dip in ε_{Nd} (Figures 5a and 5b) with values similar to that from sediments of the western Bay of Bengal during LGM [*Tripathy et al.*, 2011]. Potential sources that can contribute to the Sr and Nd excursions during LGM are relative increase in (1) Himalayan sediments and/or (2) Peninsular granites/gneisses, both of which are characterized by higher radiogenic Sr and low ε_{Nd} composition.

[27] It is known that during LGM there was decrease in SW monsoon precipitation and increase in NE monsoon [*Herzschuh*, 2006]. The intensification of NE monsoon with concomitant decrease in SW monsoon during LGM would promote strengthening of southwestward East Indian Coastal Current (EICC) in the Bay of Bengal. This in turn would enhance the flow of waters from the Bay of Bengal to the Arabian Sea [*Schott and McCreary*, 2001; *Shankar et al.*, 2002]. Such enhanced transport of Bay of Bengal waters to the southeastern Arabian Sea during LGM is documented in the oxygen isotopic composition of foraminifera deposited during this period [*Sarkar et al.*, 1990; *Tiwari et al.*, 2005].

[28] The observation that the isotopic composition of LGM stratum in SS-3101G is similar to those in western Bay of Bengal [*Tripathy et al.*, 2011], that there is enhanced flow of low salinity water from Bay of Bengal to southeastern Arabian Sea during this period and that the existence of sediment plumes in the coastal and open Bay of Bengal [*Sridhar et al.*, 2008a, 2008b; *Rajawat et al.*, 2005] is an indication that sediments from the western Bay of Bengal may be transported to this core site. However, clay mineral studies of sediments from southeastern Arabian Sea have yielded divergent conclusions; *Kessarkar et al.* [2003] suggest that the sediments of the southeastern Arabian Sea largely represent hinterland flux and are not influenced by sediments transported from the Bay of Bengal waters during the intensification of NE monsoon. In contrast, *Chauhan and Gujar* [1996]

and *Chauhan et al.* [2010] argue in favor of sediment transport from Bay of Bengal during intensification of NE monsoon.

[29] If sediments from the western Bay of Bengal are indeed the cause of Sr and Nd isotopic excursion, then based on a two end-member mixing model, it can be estimated that during LGM about one-fifth of sediments in SS-3101G are from western Bay of Bengal, the balance being of SS-3104G composition.

[30] Alternatively, considerably enhanced contribution of sediments sourced from Peninsular granites/gneisses (e.g., through the Nethravathi, Periyar rivers; Table 1) can also explain the isotopic excursions. This however seems unlikely considering that at present these rivers account for only a very small fraction of sediments to the southeastern region of the Arabian Sea [*Chandramohan and Balchand*, 2007, *Nair et al.*, 2003, *Panda et al.*, 2011] and the observation of *Ramaswamy and Nair* [1989] that much of sediments from the peninsular rivers are retained in the western shelf of India peninsula.

4.2.2. Provenance of Sediments During Holocene Intensified Monsoon Phase (IMP)

[31] The core SS-3101G shows a second excursion in Sr and Nd isotopic composition during ~9 ka, coinciding with higher SW monsoon precipitation phase commonly known as the Holocene Intensified Monsoon Phase (IMP) [*Fleitmann et al.*, 2003; *Herzschuh*, 2006; *Prell and Kutzbach*, 1987]. Based on the mixing diagram (Figure 6), this excursion also require enhanced contribution of sediments with more radiogenic Sr and unradiogenic Nd analogous to that needed to explain the LGM data. This requirement is intriguing considering that the monsoon trend was opposite during the two periods; SW monsoon being intense during ~9 ka whereas, NE monsoon was more pronounced during ~20 ka. More intense SW monsoon during Holocene IMP would constrain the North-East monsoon current (Figure 1) and therefore ensuing flow of water from the Bay of Bengal to the Arabian Sea. In such a case, supply of sediments from the Bay of Bengal to the Arabian Sea to account for the isotopic excursion at ~9 ka would also be restricted. Further, as was the case during LGM, peninsular rivers as a major source also seems unlikely unless their sediment flux during Holocene IMP was significantly higher and the sediments were transported efficiently to the core site. Two lines of evidence based on contemporary information indicate that these requirements

may not be fulfilled. These are (1) during Holocene IMP, the sea level was similar to that at present, therefore, the efficiency of shelf storage of sediments is expected to be similar to that of today [*Siddall et al.*, 2003] and (2) the clay mineralogy of sediment trap samples indicate that sediments from west flowing peninsular rivers are by and large retained in the shelf region of the Arabian Sea [*Ramaswamy and Nair*, 1989]. The Narmada and Tapi rivers are the other major suppliers of sediments to the Arabian Sea. The discharge of these rivers is dictated by SW monsoon and therefore they could transport more sediment during intensification of SW monsoon. However, these sediments cannot explain the observed magnitude in isotopic excursion if their isotopic composition was the same as those measured in this study (Table 1); the ε_{Nd} values of the Narmada and Tapi sediments are about −11.5 and −5.8 respectively, which are significantly more radiogenic than the values for core SS-3101G at Holocene IMP (−14).

[32] The Sr and Nd isotopic composition of SS-3101G display variations similar to those reported for the Indus delta during the past ~14 ka (ε_{Nd}; Figure 5d) [*Clift et al.*, 2008, 2010] with both of them showing excursions in $^{87}Sr/^{86}Sr$ and ε_{Nd} during ~9 ka. The similarity in the Sr and Nd isotopic composition and their temporal pattern hints at the possibility of supply of Indus delta sediments to the SS-3101G core site. The more radiogenic $^{87}Sr/^{86}Sr$ and lesser ε_{Nd} during ~9 ka in the core SS-3101G can be explained in terms of enhanced sediment supply through the Himalayan tributaries of the Indus. This can result from intensification of SW monsoon precipitation over the Himalaya during this period [*Clift et al.*, 2008, 2010]. The intensification of SW monsoon during ~9 ka resulted in stronger surface currents in the southeast direction from the Arabian Sea to the Bay of Bengal (Figure 1). The strengthening of this current would result in enhanced southeastward transport of water and sediments from the Arabian Sea to Bay of Bengal. The core SS-3101G lies to the east of Chagos-Laccadive ridge with the presence of sill adjacent to the core location that can facilitate transfer of sediments across the ridge by surface currents. Thus, Sr and Nd isotopic excursions observed during ~9 ka in the core SS-3101G can be a result of increased sediment supply from the Himalayan sources by the Indus tributaries. Based on the Nd isotopic data of sediments of the Indus delta, and that of the Arabian Sea sediments and two end-member mixing calculation, it can be estimated that during the Holocene IMP, about

15% of sediments at the SS-3101G location are derived from the Indus delta. This interpretation, however, rests on the premise that the sediment flux from the peninsular rivers during ~9 ka was the same as that at present and that much of the flux is retained in the shelf. If such a premise is proven to be invalid then the isotopic excursion in SS-3101G during ~9 ka may also result from sediment supply of peninsular rivers.

[33] Such a contribution from Indus at ~9 ka to core SS-3104G can be ruled out on the basis that presently, the location of the core SS-3104G is dominated by sediments brought by the Narmada and Tapi River from the Deccan basalts and Vindhyan ranges [*Kolla et al.*, 1976]. Even during the intensification of SW monsoon during ~9 ka the Deccan contribution at the core site would increase due to more rainfall on the Western Ghats and the transfer of sediments to the location of core SS-3104G.

[34] It is clear from the above discussion that in addition to climate, ocean circulation also plays an important role in sediment dispersal and their deposition as has been documented in the deposition of Meiji drift in the Pacific Ocean [*VanLaningham et al.*, 2009].

5. Conclusions

[35] Temporal variations in Sr and Nd isotopic composition of silicate component of two well dated sediment cores from the eastern Arabian Sea have been determined. Sr and Nd isotopic compositions of sediments from the more northern core (SS-3104G) display narrow ranges indicating only minor variations in their source proportion since last ~40 ka. Even the flux of aeolian dust has changed very little over the eastern Arabian Sea during last ~40 ka remaining almost consistent during this time. In contrast, the results of the southeastern Arabian Sea core (SS-3101G) exhibit two excursions in the isotopic composition coinciding with two major climate change events; LGM and Holocene Intensified Monsoon Phase (IMP). This correlation suggests significant control of climate/monsoon on erosion pattern and sedimentation. Sediment supply is controlled by climatic variability whereas its dispersal is controlled by circulation pattern of the surface ocean. The Sr and Nd isotopic excursion at ~20 ka is attributed to enhanced sediment contribution from the Bay of Bengal resulting from strengthened NE monsoon which boosts N–S coastal current in the western Bay of Bengal,

transporting water and sediments, the later with higher $^{87}Sr/^{86}Sr$ and lower ε_{Nd}. In contrast, intensified SW monsoon precipitation during ~9 ka enhanced sediment transfer from the Indus delta to the southeastern Arabian Sea enabling sediment transfer from the Arabian Sea to Bay of Bengal. This work demonstrates that the Sr and Nd isotopic composition in the silicate fraction of the Arabian Sea sediments has the potential to track the variation in the intensity and pattern of the Indian monsoon system.

References

Agnihotri, R. (2001), Chemical and isotopic studies of sediments from the Arabian Sea and Bay of Bengal, PhD thesis, Mohan Lal Sukhadia Univ., Rajasthan, India.

Agnihotri, R., M. M. Sarin, B. L. K. Somayajulu, A. J. T. Jull, and G. S. Burr (2003), Late-Quaternary biogenic productivity and organic carbon deposition in the eastern Arabian Sea, *Palaeogeogr. Palaeoclimatol. Palaeoecol.*, 197, 43–60, doi:10.1016/S0031-0182(03)00385-7.

Ahmad, S. M., G. A. Babu, V. M. Padmakumari, A. M. Dayal, B. S. Sukhija, and P. Nagabhushanam (2005), Sr, Nd isotopic evidence of terrigenous flux variations in the Bay of Bengal: Implications of monsoons during the last 34,000 years, *Geophys. Res. Lett.*, 32, L22711, doi:10.1029/2005GL024519.

Ahmad, S. M., V. M. Padmakumari, and G. A. Babu (2009), Strontium and neodymium isotopic compositions in sediments from Godavari, Krishna and Pennar rivers, *Curr. Sci.*, 97, 1766–1769.

Alagarsamy, R., and J. Zhang (2005), Comparative studies on trace metal geochemistry in Indian and Chinese rivers, *Curr. Sci.*, 89, 299–309.

Chakrabarti, R., A. R. Basu, and A. Chakrabarti (2007), Trace element and Nd-isotopic evidence for sediment sources in the mid-Proterozoic Vindhyan Basin, central India, *Precambrian Res.*, 159, 260–274, doi:10.1016/j.precamres.2007.07.003.

Chandramohan, T., and A. N. Balchand (2007), Regional sediment yield pattern for the west flowing rivers of Kerala state, India, *RMZ Mater. Geoenviron.*, 54, 501–511.

Chauhan, O. S., and A. R. Gujar (1996), Surficial clay mineral distribution on the southwestern continental margin of India: Evidence of input from the Bay of Bengal, *Cont. Shelf Res.*, 16, 321–333, doi:10.1016/0278-4343(95)00015-S.

Chauhan, O. S., A. M. Dayal, N. Basavaiah, and U. Syed Abdul Kader (2010), Indian summer monsoon and winter

hydrographic variations over past millennia resolved by clay sedimentation, *Geochem. Geophys. Geosyst.*, *11*, Q09009, doi:10.1029/2010GC003067.

Clift, P. D., J. I. Lee, P. Hildebrand, N. Shimizu, G. D. Layne, J. Blusztajn, J. D. Blum, E. Garzanti, and A. A. Khan (2002), Nd and Pb isotope variability in the Indus River System: Implications for sediment provenance and crustal heterogeneity in the Western Himalaya, *Earth Planet. Sci. Lett.*, *200*, 91–106, doi:10.1016/S0012-821X(02)00620-9.

Clift, P. D., et al. (2008), Holocene erosion of Lesser Himalaya triggered by intensified summer monsoon, *Geology*, *36*, 79–82, doi:10.1130/G24315A.1.

Clift, P. D., et al. (2010), Monsoon control over erosion patterns in the Western Himalaya: Possible feed-back into the tectonic evolution, in *Monsoon Evolution and Tectonics–Climate Linkage in East Asia*, edited by P. D. Clift, R. Tada, and H. Zheng, *Geol. Soc. Spec. Publ.*, *342*, 185–218.

Colin, C., L. Turpin, J. Bertaux, A. Desprairies, and C. Kissel (1999), Erosional history of the Himalayan and Burman ranges during the last tow glacial-interglacial cycles, *Earth Planet. Sci. Lett.*, *171*, 647–660, doi:10.1016/S0012-821X(99)00184-3.

Das, A., S. Krishnaswami, M. M. Sarin, and K. Pande (2005), Chemical weathering in the Krishna Basin and Western Ghats of the Deccan Traps, India: Rates of basalt weathering and their controls, *Geochim. Cosmochim. Acta*, *69*, 2067–2084, doi:10.1016/j.gca.2004.10.014.

Fleitmann, D., S. J. Burns, M. Mudelsee, U. Neff, J. Kramers, A. Mangini, and A. Matter (2003), Holocene forcing of the Indian monsoon recorded in a stalagmite from southern Oman, *Science*, *300*, 1737–1739, doi:10.1126/science.1083130.

Garzanti, E., G. Vezzoli, S. Andò, P. Paparella, and P. D. Clift (2005), Petrology of Indus River sands: A key to interpret erosion history of the Western Himalayan Syntaxis, *Earth Planet. Sci. Lett.*, *229*, 287–302, doi:10.1016/j.epsl.2004.11.008.

Gupta, A. K., D. M. Anderson, and J. T. Overpeck (2003), Abrupt changes in the Asian southwest monsoon during the Holocene and their links to the North Atlantic Ocean, *Nature*, *421*, 354–357, doi:10.1038/nature01340.

Gupta, H., G. J. Chakrapani, K. Selvaraj, and S.-J. Kao (2011), The fluvial geochemistry, contributions of silicate, carbonate and saline–alkaline components to chemical weathering flux and controlling parameters: Narmada River (Deccan Traps), India, *Geochim. Cosmochim. Acta*, *75*, 800–824, doi:10.1016/j.gca.2010.11.010.

Harris, N. B. W., M. Santosh, and P. N. Taylor (1994), Crustal evolution in South India: Constraints from Nd isotopes, *J. Geol.*, *102*, 139–150, doi:10.1086/629659.

Harrison, S. P., K. E. Kohfeld, C. Roelandt, and T. Claquin (2001), The role of dust in climate changes today, at the last glacial maximum and in the future, *Earth Sci. Rev.*, *54*, 43–80, doi:10.1016/S0012-8252(01)00041-1.

Herzschuh, U. (2006), Palaeo-moisture evolution in monsoonal Central Asia during the last 50,000 years, *Quat. Sci. Rev.*, *25*, 163–178, doi:10.1016/j.quascirev.2005.02.006.

Innocent, C., N. Fagel, and C. Hillaire-Marcel (2000), Sm-Nd isotope systematics in deep-sea sediments: Clay-size versus coarser fractions, *Mar. Geol.*, *168*, 79–87, doi:10.1016/S0025-3227(00)00052-9.

Jacobsen, S. B., and G. J. Wasserburg (1980), Sm-Nd isotopic systematics of chondrites and achondrites, *Meteoritics*, *15*(4), 307–308.

Kale, V. S., S. Mishra, and V. R. Baker (2003), Sedimentary records of palaeofloods in the bedrock gorges of the Tapi and Narmada rivers, central India, *Curr. Sci.*, *84*, 1072–1079.

Kessarkar, P. M., V. Purnachandra Rao, S. M. Ahmad, and G. Anil Babu (2003), Clay minerals and Sr-Nd isotopes of the sediments along the western margin of India and their implication for sediment provenance, *Mar. Geol.*, *202*, 55–69, doi:10.1016/S0025-3227(03)00240-8.

Kolla, V., L. Henderson, and P. E. Biscaye (1976), Clay mineralogy and sedimentation in the Western Indian Ocean, *Deep Sea Res.*, *23*, 949–961.

Mahoney, J. J., H. C. Sheth, D. Chandrasekharam, and Z. X. Pemg (2000), Geochemistry of flood basalts of the Toranmal section, northern Deccan traps, India: Implications for regional Deccan stratigraphy, *J. Petrol.*, *41*, 1099–1120, doi:10.1093/petrology/41.7.1099.

Milliman, J. D., G. S. Quraishee, and M. A. A. Beg (1984), Sediment discharge from the Indus river to the ocean: Past, present and furture, in *Marine Geology and Oceanography of Arabian Sea and Coastal Pakistan*, edited by B. U. Haq and J. D. Milliman, pp. 65–70, Van Nostrand Reinhold, New York.

Nair, M., T. Joseph, K. K. Balachandran, K. K. C. Nair, and J. S. Paimpillii (2003), Arsenic enrichment in estuarine sediments-impact of iron and manganese mining, in *Fate of Arsenic in the Environment (International Symposium on Fate of Arsenic in the Environment)*, edited by M. F. Ahmed, M. A. Ali, and Z. Adeel, pp. 57–67, Dhaka, Bangladesh.

Panda, D. K., A. Kumar, and S. Mohanty (2011), Recent trends in sediment load of the tropical (Peninsular) river basins of India, *Global Planet. Change*, *75*, 108–118, doi:10.1016/j.gloplacha.2010.10.012.

Peng, Z. X., J. J. Mahoney, P. R. Hooper, J. D. Macdougall, and P. Krishnamurthy (1998), Basalts of the northeastern Deccan Traps, India: Isotopic and elemental geochemistry and relation to southwestern Deccan stratigraphy, *J. Geophys. Res.*, *103*, 29,843–29,865, doi:10.1029/98JB01514.

Petit, J. R., et al. (1999), Climate and atmospheric history of the past 420,000 years form the vostok ice core, Antarctica, *Nature*, *399*, 429–436, doi:10.1038/20859.

Peucat, J. J., P. Vidal, J. Bernard-Griffiths, and K. C. Condie (1989), Sr, Nd, and Pb isotopic systematics in the Archean low to high-grade transition zone of southern India: Synaccretion vs. Post-accretion granulites, *J. Geol.*, *97*, 537–549, doi:10.1086/629333.

Prell, W. L., and J. E. Kutzbach (1987), Monsoon variability over the past 150 000 years, *J. Geophys. Res.*, *92*, 8411–8425, doi:10.1029/JD092iD07p08411.

Rahaman, W., S. K. Singh, R. Sinha, and S. K. Tandon (2009), Climate control on erosion distribution over the Himalaya during the past ~100 ka, *Geology*, *37*, 559–562, doi:10.1130/G25425A.1.

Rajawat, A. S., Y. Gupta, Y. Pradhan, A. V. Thomaskutty, and S. Nayak (2005), Coastal Processes along the Indian Coast—Case studies based on synergistic use of IRS-P4 OCM IRS-1C/1D data, *Indian J. Mar. Sci.*, *34*, 459–472.

Ramaswamy, V., and R. R. Nair (1989), Lack of cross-shelf transport of sediments on the western margin of India: Evidence from clay mineralogy, *J. Coastal Res.*, *5*, 541–546.

Ramaswamy, V., and R. R. Nair (1994), Fluxes of material in the Arabian Sea and Bay of Bengal—Sediment trap studies, in *Biogeochemistry of the Arabian Sea: Present Information and Gaps*, vol. 103, edited by D. Lal, pp. 189–210, Indian Acad. of Sci., Bangalore.

Rao, V. P., and B. R. Rao (1995), Provenance and distribution of clay minerals in the sediments of the western continental shelf and slope of India, *Cont. Shelf Res.*, *15*, 1757–1771, doi:10.1016/0278-4343(94)00092-2.

Reichart, G. J., M. den Dulk, H. J. Visser, C. H. d. Weijden, and W. J. Zachariasse (1997), A 225 kyr record of dust supply, paleoproductivity and the oxygen minimum zone from the Murray Ridge (northern Arabian Sea), *Palaeogeogr. Palaeoclimatol. Palaeoecol.*, *134*, 149–169, doi:10.1016/S0031-0182(97)00071-0.

Rutberg, R. L., S. L. Goldstein, S. R. Hemming, and R. F. Anderson (2005), Sr isotope evidence for sources of terrigenous sediments in the southeast Atlantic Ocean: Is there increased available Fe for enhanced glacial productivity?, *Paleoceanography*, *20*, PA1018, doi:10.1029/2003PA000999.

Sarkar, A., R. Ramesh, S. K. Bhattacharya, and G. Rajagopalan (1990), Oxygen isotope evidence for a stronger winter monsoon current during the last glaciation, *Nature*, *343*, 549–551, doi:10.1038/343549a0.

Sarkar, A., R. Ramesh, B. L. K. Somayajulu, R. Agnihotri, A. J. T. Jull, and G. S. Burr (2000), High resolution Holocene monsoon record from the eastern Arabian Sea, *Earth Planet. Sci. Lett.*, *177*, 209–218, doi:10.1016/S0012-821X(00)00053-4.

Schott, F. A., and J. P. McCreary Jr. (2001), The monsoon circulation of the Indian Ocean, *Prog. Oceanogr.*, *51*, 1–123, doi:10.1016/S0079-6611(01)00083-0.

Shankar, D., P. N. Vinayachandran, and A. S. Unnikrishnan (2002), The monsoon currents in the north Indian Ocean, *Prog. Oceanogr.*, *52*, 63–120, doi:10.1016/S0079-6611(02)00024-1.

Siddall, M., E. J. Rohling, A. Almogi-Labin, C. Hemleben, D. Meischner, I. Schmelzer, and D. A. Smeed (2003), Sea-level fluctuations during the last glacial cycle, *Nature*, *423*, 853–858, doi:10.1038/nature01690.

Singh, S. K., S. K. Rai, and S. Krishnaswami (2008), Sr and Nd isotopes in river sediments from the Ganga Basin: Sediment provenance and spatial variability in physical erosion, *J. Geophys. Res.*, *113*, F03006, doi:10.1029/2007JF000909.

Sinha, A., K. G. Cannariato, L. D. Stott, and H.-C. Li (2005), Variability of Southwest Indian summer monsoon precipitation during the Bølling-Allerød, *Geology*, *33*, 813–816, doi:10.1130/G21498.1.

Sirocko, F. (1995), Abrupt change in monsoonal climate: Evidence from the geochemical composition of Arabian sea sediments, habilitation thesis, Univ. of Kiel, Kiel, Germany.

Sirocko, F., and M. Sarnthein (1989), Wind-borne deposits in the northwestern Indian Ocean: Record of Holocene sediments versus modern satellite data, in *Paleoclimatology and Paleometeorology:Modern and Past Patterns of Global Atmospheric Transport*, *NATO ASI Ser., Ser. C*, edited by M. Leinen and M. Sarnthein, pp. 401–433, Kluwer Acad., Dordrecht, Netherlands.

Sirocko, F., D. G. Schonberg, and C. Devey (2000), Processes controlling trace element geochemistry of Arabian Sea sediments during the last 25,000 years, *Global Planet. Change*, *26*, 217–303, doi:10.1016/S0921-8181(00)00046-1.

Somayajulu, B. L. K., R. Bhushan, A. Sarkar, G. S. Burr, and A. J. T. Jull (1999), Sediment deposition rates on the continental margins of the eastern Arabian Sea using ^{210}Pb, ^{137}Cs and ^{14}C, *Sci. Total Environ.*, *237–238*, 429–439, doi:10.1016/S0048-9697(99)00155-2.

Sridhar, A. (2008), Evidence of a late-medieval mega flood event in the upper reaches of the Mahi River basin, Gujarat, *Curr. Sci.*, *96*, 1517–1520.

Sridhar, P. N., M. M. Ali, P. Vedamony, M. T. Babu, I. V. Ramana, and B. Jayakumar (2008a), Seasonal occurrence of unique sediment plume in the Bay of Bengal, *Eos Trans. AGU*, *89*(3), 22, doi:10.1029/2008EO030002.

Sridhar, P. N., I. V. Ramana, M. M. Ali, and B. Veeranarayana (2008b), Understanding the suspended sediment dynamics in the coastal waters of the Bay of Bengal using high resolution ocean colour data, *Curr. Sci.*, *94*, 1499–1502.

Tiwari, M., R. Ramesh, B. L. K. Somayajulu, A. J. T. Jull, and G. S. Burr (2005), Early deglacial (~19–17 ka) strengthening of the northeast monsoon, *Geophys. Res. Lett.*, *32*, L19712, doi:10.1029/2005GL024070.

Tripathy, G. R. (2011), Isotope geochemistry of black shales and recent marine sediments, PhD thesis, Mohan Lal Sukhadia Univ., Rajasthan, India.

Tripathy, G. R., S. K. Singh, R. Bhushan, and V. Ramaswamy (2011), Sr-Nd isotope composition of the Bay of Bengal sediments: Impact of climate on erosion in the Himalaya, *Geochem. J.*, *45*, 175–186.

VanLaningham, S., N. G. Pisias, R. A. Duncan, and P. D. Clift (2009), Glacial–interglacial sediment transport to the Meiji Drift, northwest Pacific Ocean: Evidence for timing of Beringian outwashing, *Earth Planet. Sci. Lett.*, *277*, 64–72, doi:10.1016/j.epsl.2008.09.033.

Wyrtki, K. (1973), Physical oceanography of the Indian Ocean, in *The Biology of the Indian Ocean*, edited by B. Zeitschel, pp. 18–36, Springer, Berlin, doi:10.1007/978-3-642-65468-8_3.